

See discussions, stats, and author profiles for this publication at: <https://www.researchgate.net/publication/40044024>

Investigation of Ethynylfurans Using the Electron Propagator Theory

ARTICLE *in* THE JOURNAL OF PHYSICAL CHEMISTRY A · DECEMBER 2009

Impact Factor: 2.69 · DOI: 10.1021/jp9061626 · Source: PubMed

CITATIONS

3

READS

234

2 AUTHORS:



Raman K. Singh

University of Yamanashi

15 PUBLICATIONS 64 CITATIONS

SEE PROFILE



Manoj Mishra

Cranfield University

83 PUBLICATIONS 447 CITATIONS

SEE PROFILE

Investigation of Ethynylfurans Using the Electron Propagator Theory

Raman K. Singh and Manoj K. Mishra*

Department of Chemistry, Indian Institute of Technology Bombay, Powai-400 076 India

Received: July 1, 2009; Revised Manuscript Received: October 31, 2009

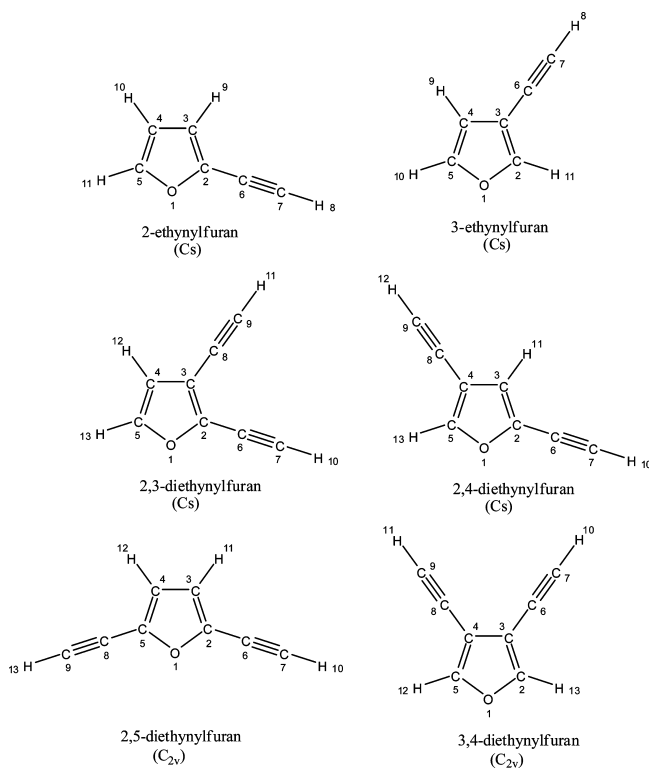
The first eleven vertical ionization energies of mono and diethynylfurans have been calculated using various electron propagator decouplings. Among all ethynylfurans, the π -orbital interactions between ethynyl and furan moieties are found to be strongest in 2,5-diethynylfuran. Oxygen atom of the furan ring and carbon atoms of ethyne group play important role in stabilization/destabilization of HOMO/LUMO of ethynylfurans. Our results for energetic stability, dipole moment, HOMO–LUMO gap, ionization energies, and electron affinity indicate that 2-ethynylfuran among monoethynylfurans and 2,5-diethynylfuran among ethynylfurans may be useful precursors for the preparation of conducting polymers.

1. Introduction

Furan is one of the fundamental heteroaromatic compounds and plays an exceptionally significant role in numerous fields of contemporary chemistry, biochemistry, and biotechnology. The structural unit of furan fits into various natural products and molecules with biochemical/pharmaceutical significance and its derivatives serve as building blocks for the synthesis of complex heteroatomic molecules and conducting polymers.^{1,2} Recently, conjugated conducting polymers have attracted much attention as novel materials due to their potential for applications in electronic and optoelectronic devices.^{3,4} Among numerous conjugated polymers, ethynylfurans have received much interest^{1–5} as a potential new material with favorable nonlinear optical (NLO) response characteristics, easy processability, and large electrical conductivity.

In this article, we focus on ethynylfuran monomers. Their electrical conductivity depends on electronic structure parameters such as ionization energy, electron affinity and band gap. An attempt at structural understanding of ethynylfuran monomers from first principles had been made by Novak et al.⁵ by recording the ultraviolet photo-electron ionization spectrum (PES) of two isomeric monoethynylfurans and three isomeric diethynylfurans. Because of strong overlap between PES bands, the recorded spectra do not give well resolved peaks, especially for states having ionization energies greater than 13 eV. MO eigenvalues and eigenvectors from Hartree–Fock (HF) calculations using 6-31 g(d,p) basis set, have been used by the same researchers⁵ for PES band assignments. The shortcomings of Koopmans' theory⁶-based interpretation of PES are well-known and use of reliable correlated ab initio techniques to supplement and interpret the photoelectron spectral (PES) data of ethynylfurans is therefore of obvious interest and importance. While a large corpus of work exists on application of EPT decouplings^{7–20} to large molecules,^{21–24} despite extensive industrial interest in ethynylfurans, to the best of our knowledge theoretical studies are rather few.⁵ This has prompted us to attempt a systematic and comprehensive study of ethynylfurans (Scheme 1) using different EPT approximants and to collate a detailed characterization of the structural properties for these potentially

SCHEME 1: Molecular Structure of Monoethynylfurans and Diethynylfurans



important compounds as a natural extension of our recent work on organic molecules.^{25–28}

The electron propagator method is well established,^{7–20} and only a skeletal outline with some computational details are offered in the next section. Results are discussed in Section 3 and a brief summary of major results concludes this paper.

2. Method

Electron propagator calculations for vertical electron detachment and attachment energies are based on the Dyson equation.^{15–19} The Dyson equation governing all electron propagator decouplings may be rewritten in the form of one-electron equations such that

* To whom correspondence should be addressed. E-mail: mmishra@iitb.ac.in.

$$[\hat{f} + \hat{\Sigma}(\varepsilon_i)]\phi_i^{\text{Dyson}}(x) = \varepsilon_i\phi_i^{\text{Dyson}}(x) \quad (1)$$

where \hat{f} is the one-electron Hartree–Fock (HF) operator and $\hat{\Sigma}(\varepsilon)$ is an energy-dependent nonlocal operator, the so-called self-energy. This operator describes electron correlation and orbital relaxation effects that are neglected by the Hartree–Fock operator, \hat{f} . Eigenfunctions of eq 1 are the Dyson orbitals, ϕ_i^{Dyson} . For electron binding energies, the Dyson orbitals are given by

$$\phi_i^{\text{IP,Dyson}}(x_N) = \sqrt{N} \int \Psi_N(x_1, x_2, x_3, \dots, x_N) \Psi_{i,N\pm 1}^*(x_1, x_2, x_3, \dots, x_{N\pm 1}) dx_1 dx_2 \dots dx_{N\pm 1} \quad (2)$$

Here, $\Psi_N(x_1, \dots, x_N)$ is the wave function for the N -electron, initial state and $\Psi_{i,N\pm 1}(x_1, \dots, x_{N\pm 1})$ is the wave function for the i -th final state with $N \pm 1$ electrons. In both expressions, x_j represents the space-spin coordinates of electron j . The eigenvalues, ε_i , of the Dyson equation correspond to electron binding energies of the molecular system. By using perturbative arguments, one may justify neglect of off-diagonal matrix elements of the self-energy operator in the HF basis. This leads to the simpler quasi-particle expression, also called the diagonal approximation.^{12–19} Thus, the electron binding energies in the quasi-particle approximation read $\varepsilon_i^{\text{HF}} + \Sigma_{ii}(E) = E$, where $\varepsilon_i^{\text{HF}}$ is the i -th canonical, HF orbital energy. All EPT methods used in this paper are based on this class of approximation, namely, diagonal second and third order, P3 and OVGf.^{7–15,18–20} The pole strength, p_i , is a good indicator of the qualitative validity of this approximation and is defined as

$$p_i = \int |\phi_i^{\text{Dyson}}(x)|^2 dx \quad (3)$$

The Dyson orbital^{15–19} within the diagonal approximation is simply proportional to a normalized, canonical HF orbital such that

$$\phi_i^{\text{Dyson}}(x) = \sqrt{p_i} \psi_i^{\text{HF}}(x) \quad (4)$$

Thus, the pole strength takes values between zero and unity. If the ionization process is well described by a Koopmans (frozen-orbital) picture, pole strengths are very close to 1.0. When pole strengths are less than 0.85, nondiagonal analysis of energy poles is required. All pole strengths in this work exceed 0.85. Those that are below 0.85 are less reliable and the corresponding electron binding energies are denoted by asterisks in the tables.

All computations were performed using the Gaussian03 suite of programs.²⁹ Geometry optimizations for ethynylfurans presented here were performed using density functional theory (DFT) with B3LYP as the exchange-correlation functional³⁰ and the 6-311++g(3df,3p) basis set. 2-Ethynylfuran, 3-ethynylfuran, 2,4-diethynylfuran, and 2,3-diethynylfuran have C_s symmetry while 2,5-diethynylfuran and 3,4-diethynylfuran have C_{2v} symmetry. Vibrational frequency calculations were also performed to confirm the stability of the optimized geometries. The Dyson orbital pictures presented in the tables were created with GaussView, and an isosurface value of 0.02 was used to produce these figures.

3. Results and Discussion

To establish the geometrical attributes of 2-ethynylfuran, 3-ethynylfuran, 2,3-diethynylfuran, 2,4-diethynylfuran, 2,5-diethynylfuran, and 3,4-diethynylfuran, we optimized geometries at B3LYP/6-311++g(3df,3p) DFT level with symmetry restrictions as shown in Scheme 1. The optimized geometries are

TABLE 1: DFT (B3LYP) Total Energies (hartree) with Zero-Point Energy Corrections, Relative Energies (kcal/mol), and Dipole Moments

| system | total energy (hartree) | relative energies (kcal/mol) | dipole moment (debye) |
|-----------------------|------------------------|------------------------------|-----------------------|
| (a) Monoethynylfurans | | | |
| 2-ethynylfuran | −306.199662 | 0.00 | 1.07 |
| 3-ethynylfuran | −306.198621 | 0.65 | 0.47 |
| (b) Diethynylfurans | | | |
| 2,3-diethynylfuran | −382.362177 | 0.69 | 0.68 |
| 2,4-diethynylfuran | −382.361844 | 0.87 | 0.35 |
| 2,5-diethynylfuran | −382.363242 | 0.00 | 1.10 |
| 3,4-diethynylfuran | −382.360195 | 1.91 | 0.24 |

planar and their standard orientations are provided in Supporting Information. The DFT total energy (hartree) with zero-point energy corrections, relative energies (kcal/mol), and dipole moments of ethynylfurans are collected in Table 1. These results demonstrate that proximity of electron acceptor ethynyl group to oxygen atom facilitates delocalization and thereby stability of ethynylfurans studied here, and we anticipate that the 2-ethynylfuran and 2,5-diethynylfuran should be most stable with most delocalized highest occupied molecular orbital (HOMO) and therefore, lowest ionization energy as required for superior conductivity. Table 1 lends credence to this anticipation and also shows that 2-ethynylfuran and 2,5-diethynylfuran have the largest dipole moment among monoethynylfurans and diethynylfurans, respectively. This indicates the possibility of these two compounds being suitable candidates for use in nonlinear optical device.

Band gap is another important parameter that governs the electrical conductivity of conjugated polymers. We have chosen to use the DFT HOMO–lowest unoccupied molecular orbital (LUMO) gap because (i) it has been found to offer better agreement with experimental values by Zhang et al.³¹ and seems to be the preferred measure of band gap in electrochemical response literature³² and (ii) sensitivity of virtual orbitals to basis set variations in HF based methods is avoided by using DFT HOMO–LUMO gap. As an indicator of band gap, we have therefore presented the DFT/B3LYP HOMO–LUMO gaps in Figure 1. It is interesting to note that the HOMO and LUMO of 2-ethynylfuran are destabilized and stabilized by 0.2 and 0.3 eV, respectively, as compared to the corresponding orbitals of 3-ethynylfuran. As a result, the 2-ethynylfuran HOMO–LUMO

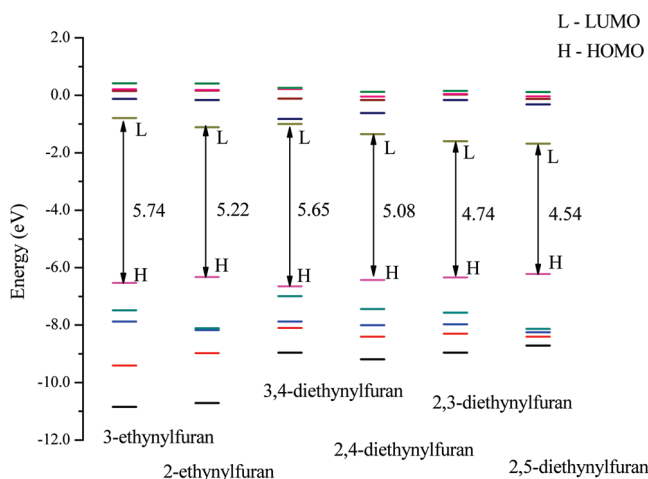
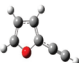




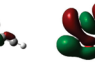
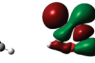


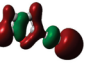
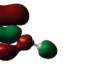



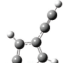




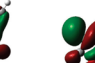



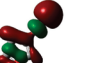


Figure 1. DFT/B3LYP HOMO–LUMO gap of monoethynylfurans and diethynylfurans.

TABLE 2: Vertical Ionization Energies of 2-Ethynylfuran and the Corresponding Dyson Orbitals

| | HOMO | HOMO-1 | HOMO-2 | HOMO-3 | HOMO-4 | HOMO-5 | HOMO-6 | HOMO-7 | HOMO-8 | HOMO-9 | HOMO-10 |
|---|---|---|---|---|---|---|--|---|---|---|---|
|  |  |  |  |  |  |  |  |  |  |  |  |
| | A'' | A'' | A' | A'' | A' | A' | A' | A' | A'' | A' | A' |
| KT | 8.42 | 11.02 | 11.19 | 12.25 | 15.23 | 15.74 | 16.16 | 17.59 | 17.69* | 19.48 | 20.79 |
| 2 nd Order | 8.38 | 10.08 | 10.68 | 11.27 | 12.51 | 13.14 | 14.05 | 15.01* | 14.17* | 17.01* | 17.34 |
| 3 rd Order | 8.61 | 10.72 | 10.96 | 11.80 | 14.41 | 14.79 | 15.03 | 16.63 | 16.38* | 18.04* | 19.46 |
| OVGF | 8.55 | 10.41 | 10.89 | 11.51 | 13.66 | 14.15 | 14.59 | 15.86 | 15.48* | 18.01* | 18.52 |
| P3 | 8.78 | 10.64 | 11.06 | 11.76 | 13.78 | 14.22 | 14.78 | 16.09 | 15.41* | 17.60 | 18.57* |
| Expt ⁵ | 8.50 | 10.28 | 10.70 | 11.28 | 13.25 | 13.90 | | | | | |

* Pole strength less than 0.85.

TABLE 3: Vertical Ionization Energies of 3-Ethynylfuran and the Corresponding Dyson Orbitals

| | HOMO | HOMO-1 | HOMO-2 | HOMO-3 | HOMO-4 | HOMO-5 | HOMO-6 | HOMO-7 | HOMO-8 | HOMO-9 | HOMO-10 |
|---|---|---|---|---|---|---|--|---|---|---|---|
|  |  |  |  |  |  |  |  |  |  |  |  |
| | A'' | A'' | A' | A'' | A' | A' | A' | A' | A'' | A' | A' |
| KT | 8.72 | 10.25 | 10.90 | 12.79 | 15.38 | 15.89 | 16.61 | 17.39 | 17.69 | 19.38 | 20.90 |
| 2 nd Order | 8.63 | 9.64 | 10.44 | 11.61 | 12.74 | 13.46 | 14.24 | 14.76* | 14.28* | 16.87 | 17.86* |
| 3 rd Order | 8.87 | 10.06 | 10.64 | 12.30 | 14.55 | 14.95 | 15.49 | 16.40 | 16.32 | 17.98 | 19.38 |
| OVGF | 8.80 | 9.81 | 10.59 | 11.93 | 13.84 | 14.36 | 14.97 | 15.63 | 15.48 | 17.49 | 18.71* |
| P3 | 9.02 | 10.10 | 10.83 | 12.22 | 13.95 | 14.46 | 15.10 | 15.88 | 15.40 | 17.52 | 18.72* |
| Expt ⁵ | 8.95 | 9.97 | 9.97 | 10.52 | 12.05 | 12.05 | | | | | |

* Pole strength less than 0.85.

gap reduces to 5.22 eV as compared to 5.74 eV calculated for 3-ethynylfuran with sizable LUMO stabilization of 2-ethynylfuran being attributed to the increased conjugation effect resulting from the proximity of the ethynyl group to the oxygen atom of the furan ring. This is also supported by atomic charges obtained from the natural population analysis for oxygen and carbon atoms presented in Supporting Information. Among diethynylfurans, the decreasing order of HOMO–LUMO gap is as follows: 3,4-diethynylfuran (5.65 eV) > 2,4-diethynylfuran (5.08 eV) > 2,3-diethynylfurans (4.74) > 2,5-diethynylfurans (4.54 eV). This seems to show that with the addition of two ethynyl groups at different positions of furan ring, conjugation effect is more pronounced than in the furan ring with only one ethynyl group. It is also worthwhile to notice that as we move from monosubstituted ethynylfuran to disubstituted ethynylfuran, proximity of ethynyl groups to the oxygen atom of furan ring again helps conjugation and as a consequence 2,5-diethynylfuran has the highest stability and the lowest band gap among ethynylfurans.

On all these counts, 2-ethynylfuran and 2,5-diethynylfurans seem useful precursors for the preparation of conducting polymers. For detailed characterization of binding energies and Dyson orbitals of all ethynylfurans, we have performed electron propagator calculation using the geometries optimized at the B3LYP/6-311++g(3df,3p) level. The energetically highest six orbitals for 2-ethynylfuran, 3-ethynylfuran, 2,3-diethynylfuran, 2,3-diethynylfuran, and 2,5-diethynylfuran are seen to be within the experimental PES energy range investigated by Novak et al.⁵ and we have chosen highest eleven orbitals for detailed examination including those of 3,4-diethynylfuran whose photoelectron spectrum has not been reported so far.

Tables 2–7 contain EPT results for vertical electron detachment energies from different decouplings. Average absolute difference between experimental assignments and those from our calculations for the set of compounds considered here range (a) from 0.32 to 1.02 eV for Koopmans results (KT) results (b) from 0.14 to 0.31 eV for second order results, (c) from 0.14 to

0.56 eV for third order results, (d) from 0.09 to 0.21 eV for OVGF results and (e) from 0.17 to 0.39 eV for partial third order (P3) results. All in all, the average of absolute differences between experimental values and those from our calculations for the molecules considered here are 0.58 eV for KT results, 0.22 eV for second order results, 0.30 eV for third order results,, 0.14 eV for OVGF results, and 0.31 eV for P3 results. On the basis of these observations, the OVGF approximant offers closest agreement with experimental results. However, for inner orbitals where experimental assignments are missing, OVGF and P3 binding energies are very close to each other and P3 results have also been included for detailed comparison with experimental peaks.

The EPT results for vertical ionization energies and corresponding Dyson orbitals for 2-ethynylfuran and 3-ethynylfuran are collected in Tables 2 and 3, respectively. The ionization energy of 2-ethynylfuran is lower than that of 3-ethynylfuran. As we move from the first HOMO to HOMO-10 orbital, relaxation and correlation correction to KT become increasingly significant as expected. As can be seen from the results of Table 3, the degeneracy between HOMO-1 and HOMO-2 (9.97 eV) and HOMO-4 and HOMO-5 (12.05 eV) orbitals of 3-ethynylfuran seen in the results of Novak et al.⁵ is not borne out by our correlated electron propagator theory calculations. To understand this deviation from experimental assignments, we have plotted the experimental ionization energies and OVGF/P3 values for HOMO to HOMO-10 in Figure 2 and, as can be seen, the degeneracy in assignment for HOMO-1 and HOMO-2 and HOMO-4 and HOMO-5 in Novak's investigations⁵ are not required by OVGF/P3 based assignment for HOMO-1 and HOMO-2 and HOMO-4 and HOMO-5 binding energies with both OVGF and P3 converging to same values for inner orbitals.

Both 2-ethynylfuran and 3-ethynylfuran have 4 π - and 20 σ -type Dyson orbitals. HOMO, HOMO-1, HOMO-3, and HOMO-7 are of π -type and the remaining occupied Dyson orbitals are of σ -type. In the σ -type HOMO-2, electron density is more localized on ethynyl carbons with almost zero-orbital density

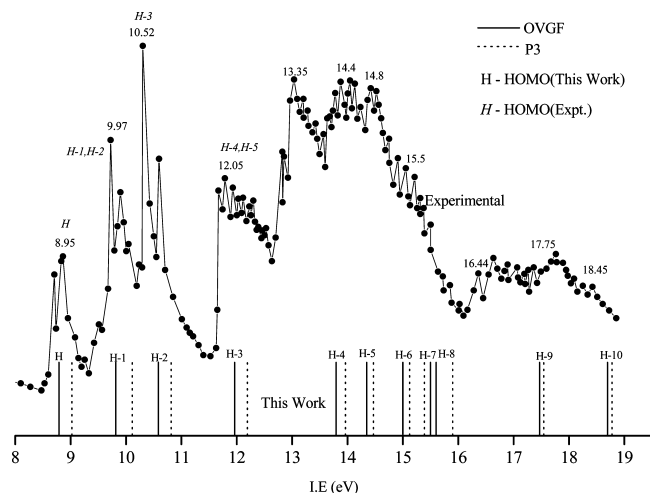


Figure 2. Comparison of OVGF and P3 results with experimental results of Novak et al. for 3-ethynylfuran.

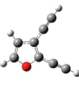

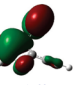
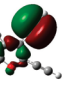
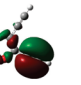


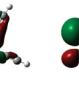
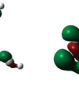
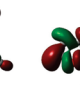


on the furan ring. The HOMO-3 orbital for both 2 and 3-ethynylfurans is predominantly π_{c-c} acetyl in nature. In σ -type HOMO-4 of both monoethynylfurans, this Dyson orbital is more localized on nonbonding O atom. The HOMO-5 to HOMO-10 orbitals of both 2- and 3-ethynylfurans have almost similar orbital topology but slightly different orientation that tracks the position of the ethyne group. The HOMO-7 Dyson orbital, having only one molecular nodal plane, has significant delocalization of electron density between ring and ethyne group. The pole strength for vertical ionization energy of the HOMO-8 is however, less than 0.85 and therefore ionization from HOMO-8 may require a multi orbital interpretation.

Tables 4 to 7 contain vertical ionization energies and corresponding Dyson orbitals for 2,3-diethynylfuran, 2,4-diethynylfuran, 2,5-diethynylfuran, and 3,4-diethynylfuran, respectively. The most stable 2,5-diethynylfuran isomer has lowest first vertical ionization energy and the least stable 3,4-diethy-

nylfuran has highest ionization energy among ethynylfurans and again as we go from the first HOMO to HOMO-10 orbital, relaxation and correlation correction to KT is increasingly more significant. As can be seen from the data of Table 6, the degeneracy between HOMO-3 and HOMO-4 (11.45 eV) of 2,5-diethynylfuran seen in the results of Novak et al.⁵ is not supported by EPT calculations. For better understanding of this difference with respect to experimental assignments, a plot of experimental ionization energies and OVGF/P3 values for HOMO to HOMO-11 is offered in Figure 3 and we see that the degenerate assignment for both HOMO-3 and HOMO-4 in Novak's investigations is not required using our assignments for HOMO-3 and HOMO-4 binding energies. Our calculations also provide description for peaks not labeled in experimental plots of both Figures 2 and 3.

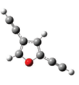

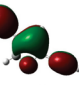

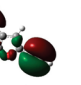

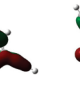
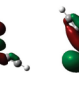
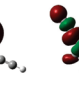
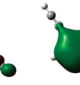
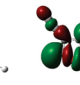

All diethynylfurans have 5π - and 25σ -type Dyson orbitals. In all these diethynylfurans HOMO, HOMO-1, HOMO-4, HOMO-5, and HOMO-10 (HOMO-9 in 2,4-diethynylfuran and 2,5-diethynylfuran) are of π -type in which four nodal planes exist for the first two HOMO/HOMO-1 Dyson orbitals and have disjointed density distribution between the ring π and acetyl π_{c-c} moieties. The HOMO-2 and HOMO-3 of Tables 4–7 are σ -type where electron density on furan ring is minimal. The HOMO-4 and HOMO-5 orbitals of all four diethynylfurans have two nodal planes including one molecular plane in which HOMO-4 Dyson orbital has large electron delocalization on the two ethynyl moieties. However, HOMO-5 orbital of all the four diethynylfurans has considerable overlap between ring and ethyne group. There is strong overlap between the π_{c-c} densities of both ethyne groups for 2,3- and 3,4-diethynylfurans while for 2,4- and 2,5-diethynylfurans, the nodal plane bisects the molecule between two halves with disjointed ethynyl π_{c-c} and ring π -electron densities. The HOMO-6 to HOMO-10 orbitals of all diethynylfurans have almost similar orbital topology but different orientation aligned with the placement of the ethynyl group. The HOMO-10 of both 2,3- and 3,4-diethynylfuran and HOMO-9 of remaining diethynylfurans has only one molecular

TABLE 4: Vertical Ionization Energies of 2,3-Diethynylfuran and the Corresponding Dyson Orbitals

| | HOMO | HOMO-1 | HOMO-2 | HOMO-3 | HOMO-4 | HOMO-5 | HOMO-6 | HOMO-7 | HOMO-8 | HOMO-9 | HOMO-10 |
|---|---|---|---|---|---|---|--|---|---|---|---|
|  |  |  |  |  |  |  |  |  |  |  |  |
| | A'' | A'' | A' | A' | A'' | A'' | A' | A' | A' | A' | A'' |
| KT | 8.38 | 10.33 | 11.01 | 11.34 | 12.05 | 13.12 | 15.69 | 16.26 | 17.11 | 17.99 | 17.99 |
| 2 nd Order | 8.26 | 9.62 | 10.43 | 10.73 | 11.33 | 11.61* | 12.61* | 13.80* | 14.18* | 15.17* | 14.32* |
| 3 rd Order | 8.52 | 10.07 | 10.67 | 11.01 | 11.60 | 12.53 | 14.87 | 15.22 | 15.89 | 16.96 | 16.55* |
| OVGF | 8.44 | 9.79 | 10.43 | 10.78 | 11.36 | 12.07 | 14.01 | 14.58 | 15.07 | 16.11 | 15.66* |
| P3 | 8.73 | 10.12 | 10.85 | 11.13 | 11.69 | 12.36 | 14.04 | 14.82 | 15.42 | 16.39 | 15.59* |
| Expt ⁵ | 8.47 | 9.82 | 10.47 | 10.71 | 11.22 | 11.87 | | | | | |

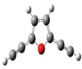


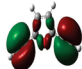
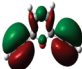




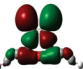

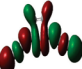
* Pole strength less than 0.85.

TABLE 5: Vertical Ionization Energies of 2,4-Diethynylfuran and the Corresponding Dyson Orbitals

| | HOMO | HOMO-1 | HOMO-2 | HOMO-3 | HOMO-4 | HOMO-5 | HOMO-6 | HOMO-7 | HOMO-8 | HOMO-9 | HOMO-10 |
|---|---|---|---|---|---|---|--|---|---|---|---|
|  |  |  |  |  |  |  |  |  |  |  |  |
| | A'' | A'' | A' | A' | A'' | A'' | A' | A' | A' | A' | A'' |
| KT | 8.50 | 10.13 | 11.02 | 11.43 | 12.47 | 12.98 | 15.77 | 16.17 | 17.36 | 18.00 | 18.04* |
| 2 nd Order | 8.37 | 9.58 | 10.50 | 10.92 | 11.47 | 11.69 | 12.69* | 13.62 | 14.40* | 15.22* | 14.39* |
| 3 rd Order | 8.61 | 9.90 | 10.70 | 11.15 | 11.98 | 12.41 | 14.93 | 15.06 | 16.03 | 16.93 | 16.55* |
| OVGF | 8.54 | 9.66 | 10.65 | 11.09 | 11.68 | 12.02 | 14.05 | 14.44 | 15.24 | 16.12 | 15.69* |
| P3 | 8.80 | 10.02 | 10.88 | 11.26 | 11.93 | 12.32 | 14.14 | 14.63 | 15.66 | 16.35 | 15.62* |
| Expt ⁵ | 8.54 | 9.78 | 10.57 | 11.13 | 11.40 | 12.00 | | | | | |

* Pole strength less than 0.85.

TABLE 6: Vertical Ionization Energies of 2,5-Diethynylfuran and the Corresponding Dyson Orbitals

| | HOMO | HOMO-1 | HOMO-2 | HOMO-3 | HOMO-4 | HOMO-5 | HOMO-6 | HOMO-7 | HOMO-8 | HOMO-9 | HOMO-10 |
|---|---|---|---|---|---|---|---|---|---|---|---|
|  |  |  |  |  |  |  |  |  |  |  |  |
| | A2 | B1 | B2 | A1 | B1 | A2 | A1 | A1 | B2 | B1 | B2 |
| KT | 8.20 | 10.90 | 11.26 | 11.45 | 12.03 | 12.82 | 15.66 | 16.20 | 16.40 | 18.07 | 18.42 |
| 2 nd Order | 8.12 | 10.22 | 10.69 | 10.87 | 10.70 | 11.83 | 12.23 | 13.66 | 14.10 | 14.26* | 15.44* |
| 3 rd Order | 8.34 | 10.60 | 10.96 | 11.11 | 11.51 | 12.27 | 15.00 | 14.97 | 15.18 | 16.51* | 17.27 |
| OVGF | 8.28 | 10.34 | 10.74 | 10.90 | 11.14 | 11.98 | 13.94 | 14.34 | 14.69 | 15.69* | 16.40 |
| P3 | 8.56 | 10.65 | 11.06 | 11.23 | 11.36 | 12.27 | 13.96 | 14.64 | 14.90 | 15.59* | 16.73 |
| Expt ⁵ | 8.28 | 10.23 | 10.72 | 11.45 | 11.45 | 11.80 | | | | | |

* Pole strength less than 0.85.

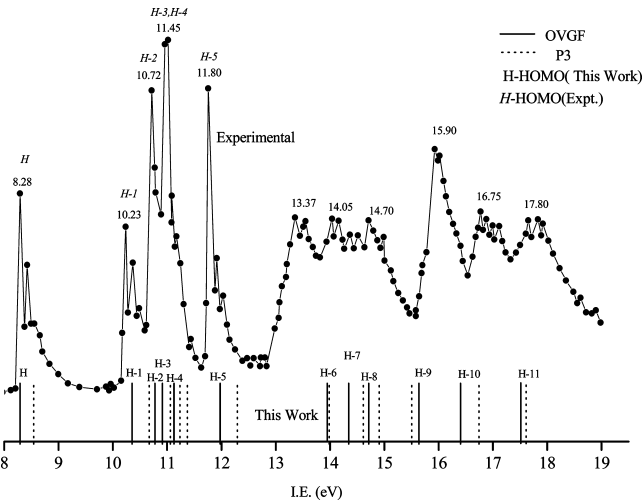


Figure 3. Comparison of OVGF and P3 results with experimental results of Novak et al. for 2,5-diethynylfuran.

nodal plane with full flow of π -electron density between the ring and both the ethynyl moieties.

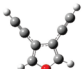

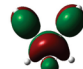

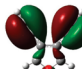


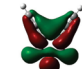
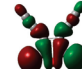

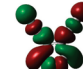

To summarize, an examination of the orbital density plots in Tables 2–7 shows that both for mono and diethynylfurans the inner orbitals are of σ -type and among HOMO to HOMO-10, (i) the π -orbitals are more loosely bound compared to σ -orbitals, (ii) the lowest π -orbital (HOMO-7 for the two monoethynylfurans and HOMO-9/HOMO-10 for the diethynylfurans) as expected is the one with only a nodal plane, (iii) as the number

of nodes increase among the π -orbitals the energy increases accordingly, and (iv) larger electron density on the electron acceptor ethynyl moiety and extended conjugation between the ethynyl moiety and the furan ring assists in easier delocalization of π -electrons and thereby stabilization (energy lowering) of these π -orbitals.

The calculated OVGF/P3 EPT ionization energies in all cases are reasonably close to the experimental values for outer valence peaks but the inner valence region beyond 13 eV is not well described. Also, since economic diagonal approximants have been utilized, the satellite shakeup peaks remain unresolved. Vertical ionization energies for HOMO-10 for all diethynylfurans except 2,5-diethynylfuran are not reliable as its pole strength is less than 0.85 and therefore a single orbital framework may not be appropriate for its interpretation. The lowest ionization energy, highest stability, and largest dipole moment among ethynylfurans indicates that the 2,5-diethynylfuran is the best potential candidate for use in preparation of high electrical conductivity polymers.

Electron affinity is another electronic parameter that indicates the kind of doping suitable for superior electrical conductivity. The electron affinity results computed from various EPT decouplings are collected in Table 8. Our OVGF/P3 results show that 2-ethynylfuran has greater electron affinity value than 3-ethynylfuran and the most stable 2,5-diethynylfuran isomer has largest electron affinity while the least stable 3,4-diethynylfuran isomer has lowest electron affinity among diethynylfurans. These electron affinities signify that conductivity of

TABLE 7: Vertical Ionization Energies of 3,4-Diethynylfuran and the Corresponding Dyson Orbitals

| | HOMO | HOMO-1 | HOMO-2 | HOMO-3 | HOMO-4 | HOMO-5 | HOMO-6 | HOMO-7 | HOMO-8 | HOMO-9 | HOMO-10 |
|---|---|---|---|---|---|---|---|---|---|---|---|
|  |  |  |  |  |  |  |  |  |  |  |  |
| | A2 | B1 | A1 | B2 | A2 | B1 | A1 | B2 | A1 | B2 | B1 |
| KT | 8.79 | 9.60 | 10.88 | 11.10 | 12.13 | 13.38 | 15.86 | 16.89 | 16.93 | 18.00 | 18.03* |
| 2 nd Order | 8.62 | 9.11 | 10.31 | 10.64 | 11.34 | 11.86 | 12.93 | 13.73 | 14.51 | 15.17 | 14.47* |
| 3 rd Order | 8.89 | 9.44 | 10.59 | 10.85 | 11.71 | 12.80 | 14.97 | 15.86 | 15.70 | 16.83 | 16.49* |
| OVGF | 8.82 | 9.35 | 10.35 | 10.79 | 11.43 | 12.34 | 14.16 | 14.92 | 15.15 | 16.04 | 15.67* |
| P3 | 9.05 | 9.59 | 10.76 | 11.02 | 11.78 | 12.63 | 14.26 | 15.22 | 15.33 | 16.38 | 15.59* |

* Pole strength less than 0.85.

TABLE 8: Electron Affinity of Ethynylfurans (eV)

| | 2-ethynylfuran | 3-ethynylfuran | 2,3-diethynylfuran | 2,4-di ethynylfuran | 2,5-diethynylfuran | 3,4-diethynylfuran |
|-----------|----------------|----------------|--------------------|---------------------|--------------------|--------------------|
| KT | 0.97 | 0.99 | 0.95 | 0.95 | 0.95 | 0.99 |
| 2nd order | 0.71 | 0.74 | 0.69 | 0.69 | 0.67 | 0.72 |
| 3rd order | 0.77 | 0.79 | 0.74 | 0.74 | 0.74 | 0.77 |
| OVGF | 0.75 | 0.78 | 0.73 | 0.73 | 0.72 | 0.76 |
| P3 | 0.72 | 0.74 | 0.70 | 0.70 | 0.68 | 0.73 |

2-ethynylfuran among monoethynylfurans and 2,5-diethynylfurans among diethynylfurans can be enhanced using a n-type dopant.

4. Concluding Remarks

The electron propagator calculations on ethynylfurans have been performed using the B3LYP/6-311++g(3df,3p) optimized geometries. The OVG/P3 vertical ionization energies in all cases are in reasonable agreement with experimental results but since only the diagonal EPT approximants have been employed, the assignments proposed for PES peaks beyond 13 eV do not correlate as well. As we move toward deeper orbitals, relaxation and correlation correction to Koopmans results become more pronounced as expected. As can be seen from the results of Table 3, the degeneracy between HOMO-1 and HOMO-2 (9.97 eV) and HOMO-4 and HOMO-5 (12.05 eV) of 3-ethynylfuran seen in the results of Novak et al.⁵ is not borne out by the EPT calculations. Similarly, the degeneracy between HOMO-3 and HOMO-4 of 2,5-diethynylfuran seen in Novak's results are not corroborated by EPT results of Table 6. Our findings therefore suggest that the photo electron spectra of these compounds need to be revisited with a reconsideration of the peak assignments and further experimental investigation is warranted. Our results we hope will also motivate further EPT investigations of the PES spectra treated here using more accurate decouplings like the third-order algebraic-diagrammatic construction approximation scheme (ADC(3))^{12,13,33} and the full two particle-one hole Tamm Dancoff approximation (2ph-TDA).^{34–36} There are no experimental results for 3,4-diethynylfuran and our predicted vertical electron detachment energies for 3,4-diethynylfuran should motivate experimental investigation of this related system.

Our examination also shows that the HOMO–LUMO gap of 2-ethynylfuran is 0.5 eV less than that of 3-ethynylfuran and 2,5-diethynylfuran has the lowest HOMO–LUMO gap among all ethynylfurans. Charges computed using natural population analysis indicate that oxygen atom of furan ring and carbon atoms of ethyne group play important role in destabilization/stabilization of HOMO/LUMOs in ethynylfurans.

2,5-Diethynylfuran is found to have the most stable structure, largest dipole moment, lowest HOMO–LUMO gap, lowest ionization energy, and lowest electron affinity among ethynylfurans. These together suggest that 2,5-diethynylfuran may be a promising potential candidate for non linear optical devices and its electrical conductivity may be further enhanced by n-type doping.

In conclusion, our computations indicate the possibility that 2-ethynylfuran among monoethynylfurans and 2,5-diethynylfuran among diethynylfurans may be useful precursors for the preparation of conducting polymers.

Acknowledgment. This research has been supported by a grant from the Department of Science and Technology, India (Grant SR/S1/PC-30/2006).

Supporting Information Available: Cartesian coordinates (in angstroms) and natural population analysis of all structures discussed in this paper. This material is available free of charge via the Internet at <http://pubs.acs.org>.

References and Notes

(1) Bredas, J. L.; Silbey, R. *Conjugated Polymers: The Novel Science and Technology of Highly Conducting and Nonlinear Optically Active Materials*; Kluwer: Dordrecht, 1991.

- (2) Katritzky, A. R.; Pozharskii, A. F. *Handbook of Heterocyclic Chemistry*; Academic Press: Amsterdam, 2000.
- (3) Roncali, J. *Chem. Rev.* **1992**, 92, 711.
- (4) Kanis, D. R.; Ratner, M. A.; Marks, T. J. *Chem. Rev.* **1994**, 94.
- (5) Novak, I.; Ng, S. C.; Jin, S.; Huang, H. H.; Huang, W. J. *Phys. Chem. A* **1997**, 101, 3501.
- (6) Koopmans, T. *Physica* **1933**, 1, 104.
- (7) Cederbaum, L. S. *J. Phys. B* **1975**, 8, 280.
- (8) Cederbaum, L. S.; Domcke, W. *Adv. Chem. Phys.* **1977**, 36, 205.
- (9) Simons, J. *Annu. Rev. Phys. Chem.* **1977**, 28, 15.
- (10) Öhrn, Y.; Born, G. *Adv. Quantum Chem.* **1981**, 13, 1.
- (11) Jørgensen, P.; Siomons, J. *Second Quantization Based Methods in Quantum Chemistry*; Academic Press: New York, 1981.
- (12) Schirmer, J.; Cederbaum, L. S.; Walter, O. *Phys. Rev. A* **1983**, 28, 1237.
- (13) Von Niessen, W.; Schirmer, J.; Cederbaum, L. S. *Comput. Phys. Rep.* **1984**, 1, 57.
- (14) Cederbaum, L. S.; Domcke, W.; Schirmer, J.; VonNiessen, W. *Adv. Chem. Phys.* **1986**, 65, 115.
- (15) Ortiz, J. V. *J. Chem. Phys.* **1996**, 104, 7599.
- (16) Mishra, M. K.; Medikeri, M. N. *Adv. Quantum Chem.* **1996**, 27, 225.
- (17) Ortiz, J. V. *Computational Chemistry: Reviews of Current Trends*; Leszczynski, J., Ed.; World Scientific: Singapore, 1997, Vol. 2, p 1.
- (18) Ortiz, J. V. *Adv. Quantum Chem.* **1999**, 33, 35.
- (19) Ortiz, J. V.; Zakrzewski, V. G.; Dolgounitchewa, O. In *Conceptual Trends in Quantum Chemistry*; Kryachko, E. S., Ed.; Kluwer: Dordrecht, 1997, Vol. 3, p 465.
- (20) Linderberg J.; Öhrn, Y. *Propagators in Quantum Chemistry*, 2nd ed.; Wiley: Hoboken, NJ, 2004.
- (21) Deleuze, M.; Cederbaum, L. S. *On the Adequacy of the one-particle Picture of Ionization for Polymers*, Second international Conference on Polymer-Solid interfaces: from Model to Real Systems, Namur, Belgium; Pireaux, J. J., Delhalle, J., Rudolf, P., Eds.; 1998; pp 77–90.
- (22) Deleuze, M.; Cederbaum, L. S. The New Challenges of the Theory of Ionization for Polymers and Solids. In *Advances in Quantum Chemistry*; Sabin, J. R., Zerner, M. C., Brandas, E., Ortiz, J. V., Kutrz, H., Eds.; Academic Press: New York, 1999, Vol. 35, pp 77–94.
- (23) Deleuze, M.; Trofimov, A. B.; Cederbaum, L. S. *J. Chem. Phys.* **2001**, 115, 5859.
- (24) Huang, Y. R.; Hajgato, B.; Ning, C. G.; Zhang, S. F.; Liu, K.; Luo, Z. H.; Deng, J. K.; Deleuze, M. S. *J. Phys. Chem. A* **2008**, 112, 2339.
- (25) Melin, J.; Mishra, M. K.; Ortiz, J. V. *J. Phys. Chem. A* **2006**, 110, 12231.
- (26) Melin, J.; Singh, R. K.; Mishra, M. K.; Ortiz, J. V. *J. Phys. Chem. A* **2007**, 111, 13069.
- (27) Singh, R. K.; Ortiz, J. V.; Mishra, M. K. *Int. J. Quantum Chem.* **2009**, 109, DOI: 10.102/qua.22363.
- (28) Singh, R. K.; Mishra, M. K. *J. Chem. Sci.* **2009**, 121 (5), 867.
- (29) Frisch, M. J.; Trucks, G. W.; Schlegel, H.; Scuseria, G. E.; Robb, M. A.; Cheeseman, J. R.; Montgomery, J. A., Jr.; Vreven, T.; Kudin, K. N.; Burant, J. C.; Millam, J. M.; Iyengar, S. S.; Tomasi, J.; Barone, V.; Mennucci, B.; Cossi, M.; Scalmani, G.; Rega, N.; Petersson, G. A.; Nakatsuji, H.; Hada, M.; Ehara, M.; Toyota, K.; Fukuda, R.; Hasegawa, J.; Ishida, M.; Nakajima, T.; Honda, Y.; Kitao, O.; Nakai, H.; Klene, M.; Li, X.; Knox, J. E.; Hratchian, H. P.; Cross, J. B.; Adamo, C.; Jaramillo, J.; Gomperts, R.; Stratmann, R. E.; Yazyev, O.; Austin, A. J.; Cammi, R.; Pomelli, C.; Ochterski, J. W.; Ayala, P. Y.; Morokuma, K.; Voth, G. A.; Salvador, P.; Dannenberg, J. J.; Zakrzewski, V. G.; Dapprich, S.; Daniels, A. D.; Strain, M. C.; Farkas, O.; Malick, D. K.; Rabuck, A. D.; Raghavachari, K.; Foresman, J. B.; Ortiz, J. V.; Cui, Q.; Baboul, A. G.; Clifford, S.; Cioslowski, J.; Stefanov, B. B.; Liu, G.; Liashenko, A.; Piskorz, P.; Komaromi, I.; Martin, R. L.; Fox, D. J.; Keith, T.; Al-Laham, M. A.; Peng, C. Y.; Nanayakkara, A.; Challacombe, M.; Gill, P. M. W.; Johnson, B.; Chen, W.; Wong, M. W.; Gonzalez, C.; Pople, J. A. *Gaussian 03*, revision C. 02; Gaussian, Inc.: Pittsburgh, PA, 2003.
- (30) Becke, A. D. *J. Chem. Phys.* **1993**, 98, 5648.
- (31) Zhange, G.; Musgrave, C. B. *J. Phys. Chem. A* **2007**, 111, 1554.
- (32) Kim, S.; Lee, J. K.; Kang, S. O.; Ko, J.; Yum, J.-H.; Fantacci, S.; Angelies, F. D.; Censo, D. D.; Nazeeruddin, M. K.; Grätzel, M. *J. Am. Chem. Soc.* **2006**, 128, 16701.
- (33) Trofimov, A. B.; Schirmer, J.; Kobychiev, V. B.; Potts, A. W.; Holland, D. M. P.; Karlsson, L. *J. Phys. B* **2006**, 39, 305.
- (34) Schirmer, J.; Cederbaum, L. S. *J. Phys. B* **1978**, 11, 1889.
- (35) Schirmer, J.; Domcke, W.; Cederbaum, L. S.; Niessen, W. V. *J. Phys. B* **1978**, 11, 1901.
- (36) Mishra, M.; Öhrn, Y. *Chem. Phys. Lett.* **1980**, 71, 1980.